JOURNAL OF BACTERIOLOGY, Mar. 1991, p. 1623–1633
0021-9193/91/051623-11$02.00/0

Vol. 173, No. 5

Freeze-Substitution of Gram-Negative Eubacteria: General Cell Morphology and Envelope Profiles

L. L. GRAHAM,[1]* R. HARRIS,[1] W. VILLIGER,[2] AND T. J. BEVERIDGE[1]

Department of Microbiology, College of Biological Sciences, University of Guelph, Guelph, Ontario, Canada N1G 2W1,[1] and Department of Microbiology, Biozentrum, University of Basel, CH-4056 Basel, Switzerland[2]

Received 15 October 1990/Accepted 17 December 1990

Freeze-substitution was performed on strains of *Escherichia coli*, *Pasteurella multocida*, *Campylobacter fetus*, *Vibrio cholerae*, *Pseudomonas aeruginosa*, *Pseudomonas putida*, *Aeromonas salmonicida*, *Proteus mirabilis*, *Haemophilus pleuropneumoniae*, *Caulobacter crescentus*, and *Leptothrix discophora* with a substitution medium composed of 2% osmium tetroxide and 2% uranyl acetate in anhydrous acetone. A thick periplasmic gel ranging from 10.6 to 14.3 nm in width was displayed in *E. coli* K-12, K30, and His 1 (a K-12 derivative containing the K30 capsule genes), *P. multocida*, *C. fetus*, *P. putida*, *A. salmonicida*, *H. pleuropneumoniae*, and *P. mirabilis*. The other bacteria possessed translucent periplasms in which a thinner peptidoglycan layer was seen. Capsular polysaccharide, evident as electron-dense fibers radiating outward perpendicular to the cell surface, was observed on *E. coli* K30 and His 1 and *P. mirabilis* cells. A more random arrangement of fibers forming a netlike structure was apparent surrounding cells of *H. pleuropneumoniae*. For the first time a capsule, distinct from the sheath, was observed on *L. discophora*. In all instances, capsular polysaccharide was visualized in the absence of stabilizing agents such as homologous antisera or ruthenium red. Other distinct envelope structures were observed external to the outer membrane including the sheath of *L. discophora* and the S layers of *A. salmonicida* A450 and *C. crescentus* CB15A. We believe that the freeze-substitution technique presents a more accurate image of the structural organization of these cells and that it has revealed complex ultrastructural relationships between cell envelope constituents previously difficult to visualize by more conventional means of preparation.

Cryopreparation of tissue for electron microscopic examination has redefined concepts of organelle distribution within eukaryotic cells (30). Ultrarapid freezing ensures that ice crystal damage to cellular constituents is minimized and leaves cells so exquisitely preserved that they may be thawed with minimal loss of viability. Freeze-substitution, a cryotechnique which combines the advantages of low-temperature methods with the ease of room temperature specimen preparation, has proved especially promising as a new method for ultrastructural preservation. In this technique, intracellular water, present as vitreous ice formed as a result of ultrarapid freezing (cryofixation), is substituted with chemical fixatives and dehydrating agents while maintained at low temperatures (−80°C) to minimize secondary ice crystal growth. The resulting biological specimens, devoid of free water, are miscible with standard plastic resins and therefore are amenable to standard thin-sectioning techniques.

To date, freeze-substitution has been only infrequently used in microbiology. Yet, the studies which have been done, especially those on bacteria, have yielded remarkable results. In *Escherichia coli*, for example, the periplasm has been preserved as a periplasmic gel (24) composed of peptidoglycan, enzymes, cell wall precursors, and exocomponents in transit, while the chromosome has been shown to exist in a noncondensed form distributed throughout most of the cytoplasmic volume (25), and recently, adhesion zones (7, 9) in nonplasmolyzed cells have been questioned as an artifactual product of standard chemical processing (29). Freeze-substitution of gram-positive eubacteria, such as *Bacillus subtilis* and *Staphylococcus aureus*, has shown the cell wall to be much thicker and fibrous in nature than originally thought (6, 22, 23, 37). In addition, freeze-substitution is the method of choice for thin-section examination of the archaeobacterium *Methanosarcina barkeri* since the polysaccharide wall has been shown to swell during standard chemical fixation (3).

It has become evident that freeze-substitution by a simple regimen of freezing and processing (23) yields superior ultrastructural detail in *B. subtilis* and *E. coli* cells compared with conventional embedding protocols providing that freezing damage is minimized (22). In the present study, we extended our freeze-substitution observations to include a diverse range of gram-negative eubacteria chosen either because they are difficult to image by conventional means or because they possess delicate, hard to preserve, additional layers external to their outer membranes (i.e., regularly structured arrays or S layers, capsules, and sheaths). We compared cell envelopes of these strains with an acapsular strain, *E. coli* K-12, whose outer membrane is well characterized and is known to possess only short core polysaccharide on its lipopolysaccharide (19, 20). A K-12 mutant strain, His 1, expressing *E. coli* K30 capsular polysaccharide (CPS) and several other encapsulated species are included to determine the fidelity of preservation of this extremely hydrated exopolymer. This is not meant to be a comparison of electron microscopic processing methods, but rather to provide a point of reference from which ultrastructural differences between conventionally embedded and freeze-substituted eubacteria may be appreciated. A detailed biochemical comparison of these two techniques using radioisotope-labeled cell components may be found elsewhere (22).

* Corresponding author.

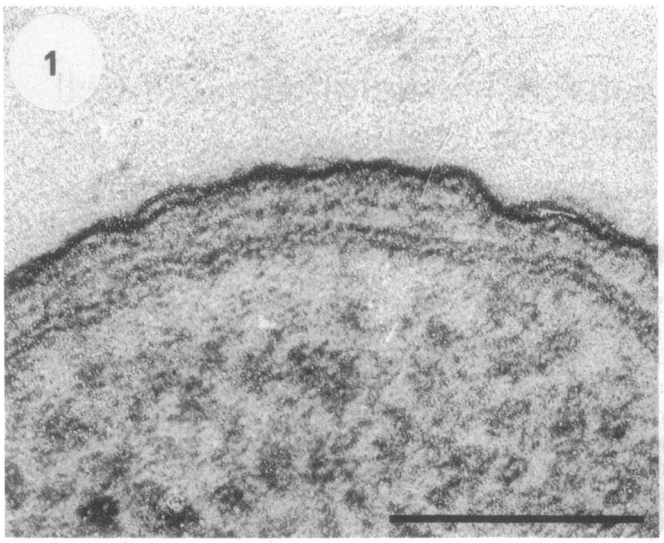

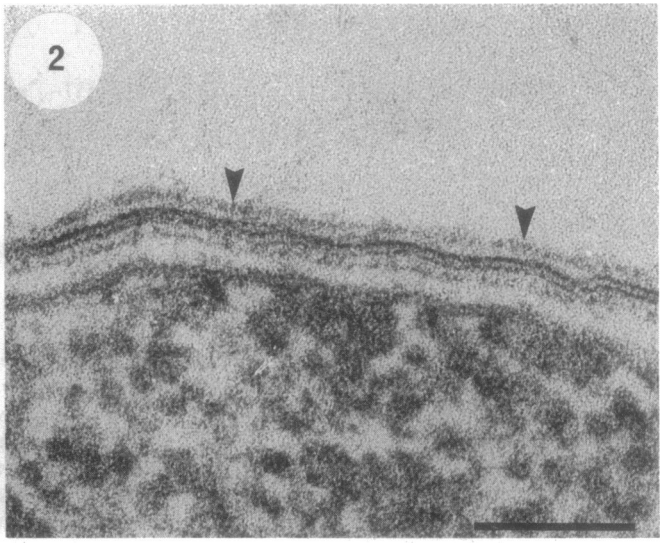

FIG. 1. Envelope profile of *E. coli* K-12 prepared by conventional embedding. Bar, 100 nm.

FIG. 2. Envelope profile of *A. salmonicida* A450 prepared by conventional embedding. Note the A-layer (an S layer) external to the outer membrane (arrowheads). Bar, 100 nm.

MATERIALS AND METHODS

Bacterial strains. Unless otherwise stated, all media were obtained from Difco. Culture conditions were selected to optimize growth for each species, and when possible, mid-exponential phase cultures were used for study. *E. coli* K-12 was grown in 50-ml volumes of nutrient broth in 125-ml flasks at 37°C and shaken at 150 rpm for 5 h (optical density at 600 nm = 0.57). *Pseudomonas putida* ATCC 17484, supplied by V. L. McKinley, Roosevelt University, Chicago, Ill., was grown for 24 h with minimal agitation in nutrient broth at room temperature (optical density at 600 nm = 1.1). *Pasteurella multocida* type D (acapsular) was supplied by M. Jacques, Université de Montréal, St. Hyacinthe, Québec, Canada. Cells were grown for 18 h at 37°C in tryptic soy broth at 150 rpm (optical density at 600 nm = 0.95). *Caulobacter crescentus* CB15A (an S-layer strain) and CB15A KSAC, an isogenic strain in which the S-layer gene has been deleted by homologous recombination, were provided by J. Smit and S. G. Walker, University of British Columbia, Vancouver, British Columbia, Canada. Cells were grown statically at 30°C for 18 h (optical density at 600 nm = 0.91) in PYE broth consisting of (per liter) 2 g of peptone, 1 g of yeast extract, 0.2 g of $MgSO_4 \cdot 7H_2O$, and 0.1 g of $CaCl_2 \cdot 2H_2O$. A culture of *Leptothrix discophora* was supplied by W. Ghiorse, Cornell University, Ithaca, N.Y. Cells were grown for 7 days as biofilms on the surface of a mineral salts medium containing $MnCl_2$. This medium (PYG) consisted of (per liter) 0.25 g of peptone, 0.25 g of yeast extract, 0.25 g of glucose, 0.6 g of $MgSO_4 \cdot 7H_2O$, 0.07 g of $CaCl_2 \cdot 2H_2O$, 0.07 g of $MnCl_2 \cdot 4H_2O$, and 0.013 g of $FeCl_3 \cdot 6H_2O$, adjusted to a pH of 7.6 with 1 M NaOH prior to autoclaving (2).

Pseudomonas aeruginosa ATCC 9027 and *Vibrio cholerae* CA401 biotype EL TOR, serotype INABA, were grown overnight at 37°C on brain heart infusion agar. *Aeromonas salmonicida* A450 (an A-layer strain) and 449 TM1, an isogenic kanamycin-resistant strain lacking the A-layer, were obtained from T. J. Trust, University of Victoria, Victoria, British Columbia, Canada, and grown for 18 h at 21°C on tryptic soy agar.

To enhance synthesis of CPS, we cultured the following strains overnight on solid media at 37°C. *E. coli* K30 and a K-12 derivative, strain His 1, containing the genes for the K30 capsule, were grown on nutrient agar. His 1 was provided by C. Whitfield, University of Guelph, Guelph, Ontario, Canada. *Proteus mirabilis* 2573, originally isolated from a patient with a struvite urinary calculus (32), was grown on brain heart infusion agar. *Haemophilus pleuropneumoniae* CM5 was provided by S. Rosendal, University of Guelph. Cells were grown on brain heart infusion agar containing 5% sheep erythrocytes and NAD at 10 mg/ml. *Campylobacter fetus* RC4 was supplied by J. Penner, University of Toronto, Toronto, Ontario, Canada. Cells were grown on brain heart infusion agar containing 5% sheep erythrocytes in an atmosphere of 5% O_2, 15% CO_2, and 80% N_2 as generated by Campy Gas Pacs (Oxoid).

Conventional embedding. All cultures were processed through the following conventional chemical fixation and embedding regimen. For this report, only *E. coli* K-12 and *A. salmonicida* A450 are shown (Fig. 1 and 2) and are representative. Cells were harvested and suspended in 2% (vol/vol) glutaraldehyde (Marivac Ltd.) in 0.05 M HEPES (*N*-2-hydroxyethylpiperazine-*N'*-2-ethanesulfonic acid; Research Organics Inc.) buffer (pH 6.8) and fixed for 2 h at room temperature. Fixed cells were pelleted, enrobed in 2% Noble agar, and cut to form blocks ca. 3 mm in length and 1 mm in diameter. Agar-bacteria blocks were washed five times for 15 min each in HEPES buffer, postfixed in 2% (wt/vol) aqueous osmium tetroxide (Fisher Scientific) for 2 h at room temperature, and washed five times in buffer. Samples were then stained en bloc in 2% (wt/vol) aqueous uranyl acetate for 2 h at room temperature and washed an additional five times. Cells were dehydrated through a graded acetone series, infiltrated overnight at room temperature in an acetone-Epon 812 mixture (1:1), embedded in fresh Epon 812 (Can EM Ltd.) and polymerized for 36 h at 60°C.

Freeze-substitution. *V. cholerae* CA401 and *A. salmonicida* A450 cells were collected by using a spatula to gently scrape cells from the agar surface and were processed by the method of Hobot et al. (25). Cells were deposited on Job no.

807S cigarette paper (punched out to a diameter of 5.5 mm), mounted, and immediately cryofixed by projection (slamming) onto a copper block cooled with liquid helium by the method of Escaig (18). Substitution was performed in pure acetone containing 2% (wt/vol) osmium tetroxide and molecular sieve (pore diameter, 0.4 nm; Perlform; Merck & Co., Inc., Rahway, N.J.) at −87°C for 80 h. Fresh substitution medium plus molecular sieve was used at each of the four succeeding steps. The temperature was gradually increased (Δt = 6.7°C/h) to −40°C and held constant for 7 h, at −40°C for 2 h, to 0°C for 2 h, and to room temperature for 1 h. Samples were washed for 30 min in acetone at room temperature and infiltrated in a graded series of Epon 812-acetone mixtures: 1:2 for 1 h, 1:1 for 1 h, 2:1 for 16 h with vial tops removed to allow acetone to evaporate, and pure Epon 812 for 3 h. Samples were embedded in fresh Epon 812 and polymerized at 45°C for 24 h and at 60°C for 4 days.

The remaining strains were processed as follows. Bacteria grown in broth culture were harvested by centrifugation (6,000 × *g*, 20 min) and washed once in 0.05 M HEPES buffer (pH 6.8) to remove contaminating medium components. Cells grown on solid media were gently scraped from the agar surface in the presence of HEPES buffer. *H. pleuropneumoniae*, *C. fetus*, and *L. discophora* cells were briefly treated with 18% (vol/vol) glycerol (Fisher Scientific) in buffer prior to cryofixation. Although glycerol has been shown to have no effect on the retention of specific cell components in *E. coli* and *B. subtilis* cells (22), we have found that it does have some cryoprotective value for certain bacteria. Cells were freeze-substituted by the method of Graham and Beveridge (22, 23). Bacteria were pelleted in an Eppendorf microcentrifuge tube, and a volume of molten 2% (wt/vol) Noble agar (ca. 60°C) equal to the cell pellet was added, mixed, and immediately spread as a thin layer (ca. 20 to 30 μm as visualized by electron microscopy) on cellulose-ester membranes (Gelman Sciences) by using a sterile glass microscope slide. *L. discophora*, which grows as a biofilm on the surface of liquid media, was freeze-substituted after carefully layering portions of an intact biofilm on a cellulose-ester filter without prior washing in buffer and securing with molten agar. Wedge-shaped portions from each of the prepared membranes were cryofixed by plunge-freezing in liquid propane (−196°C) as the cryogen and substituted in sealed glass vials at −80°C for 72 h. Substitution medium consisted of 2% (wt/vol) osmium tetroxide (Fisher Scientific) and 2% (wt/vol) uranyl acetate (Fisher Scientific) in anhydrous acetone in the presence of molecular sieve (sodium alumino silicate; pore diameter, 0.4 nm; Sigma Chemical Co.). After substitution, vials were removed and allowed to come to room temperature and samples were washed six times for 15 min each in fresh anhydrous acetone to remove excess fixative. Samples were infiltrated overnight at room temperature in an acetone-Epon 812 mixture (1:1), embedded in fresh Epon 812, and polymerized at 60°C for 36 h.

Electron microscopy. Thin sections were cut with a Reichert-Jung Ultracut E ultramicrotome and mounted on Formvar carbon-coated copper grids. In some instances, sections were poststained with 2% (wt/vol) aqueous uranyl acetate and lead citrate (35). Sections were examined in a Philips EM300 transmission electron microscope at an accelerating voltage of 60 kV under standard operating conditions with the cold trap in place.

RESULTS AND DISCUSSION

Envelope profiles of conventionally prepared cells. All representatives of the 10 genera examined in this study possessed thin-section envelope profiles typical of conventionally processed gram-negative cells with and without capsules or S layers (the envelope of *E. coli* K-12 in Fig. 1 is representative). These profiles showed a translucent periplasm bound by plasma and outer membranes. All outer membranes were wavy (e.g., *P. aeruginosa*, *P. putida*, *P. mirabilis*, *P. multocida*, *C. fetus*, *V. cholerae*, *A. salmonicida*, *H. pleuropneumoniae*, *E. coli*, *C. crescentus*, and *L. discophora*) with nodes touching a thin, 2- to 3-nm peptidoglycan layer. An accurate measurement of periplasm thickness was difficult to determine owing to the waviness of the outer membrane. Distinct capsules were not seen on any of the bacteria, although electron-dense material, presumably collapsed CPS, was visible on encapsulated strains. The S layer of *A. salmonicida*, termed the A-layer (28), was distinguished only as an additional electron-dense line 10 nm or more above the outer membrane (Fig. 2).

Earlier chemical analyses in our laboratory and others have shown that conventional processing extracts many different components from biological specimens (14–16, 22, 38). Indeed, all the strains processed by conventional chemical methods in our present study appeared to have been leached of most of their highly mobile constituents (e.g., low-molecular-weight proteins, nucleic acids, lipids, etc.) as evidenced by irregularly distributed cytoplasmic and nucleoid material and nonuniform envelope profiles.

Freeze-substituted whole cells. Examination of freeze-substituted cell preparations revealed turgid cells with complex envelope ultrastructure (Fig. 3, 4, and 5). Compared with conventionally processed cells, freeze-substituted cells showed outer and plasma membranes of uniform width as well as a peptidoglycan component present either as an electron-dense periplasmic gel 10.6 to 14.3 nm in width or as an electron-dense band 3.4 to 4.7 nm in width. In all cases, these measurements were too large to be equivalent to a monolayer of peptidoglycan (11) and therefore support the concept of a multilayered peptidoglycan. In some strains, additional structures including capsules, sheaths, or S layers were observed external to the outer membrane. All cells judged to be well frozen (i.e., those closest to the freezing edge) lacked the artifacts associated with conventional preparations of gram-negative cells, such as wavy outer membranes and voids within the cytoplasm. Dubochet et al. (17) reported minimal variation in electron density throughout the cytoplasm of thin-sectioned, frozen-hydrated bacterial cells. The uniform appearance of the cytoplasm in our cell preparations implies an even distribution of ribosomes and is indicative of accurate preservation. Distinct ribosome-free regions as reported by Hobot et al. (25) or areas of grainy and fibrous material were not observed. Preparatory methods may be responsible for this difference as the osmium-substituted *E. coli* B cells investigated by Hobot et al. (25) were slam frozen by a liquid helium-cooled system, although these characteristics were not observed in our *V. cholerae* and *A. salmonicida* cells also processed by this method.

Envelope profiles of freeze-substituted cells. (i) Outer membranes. Most outer membranes were smooth, asymmetrically stained structures (the outer face possessed more heavy-metal stain than the inner face) of uniform width bordering a periplasmic gel and were readily visualized prior to poststaining. This profile has been described previously (22–24) and Fig. 6, an *E. coli* K-12 cell, is representative (see

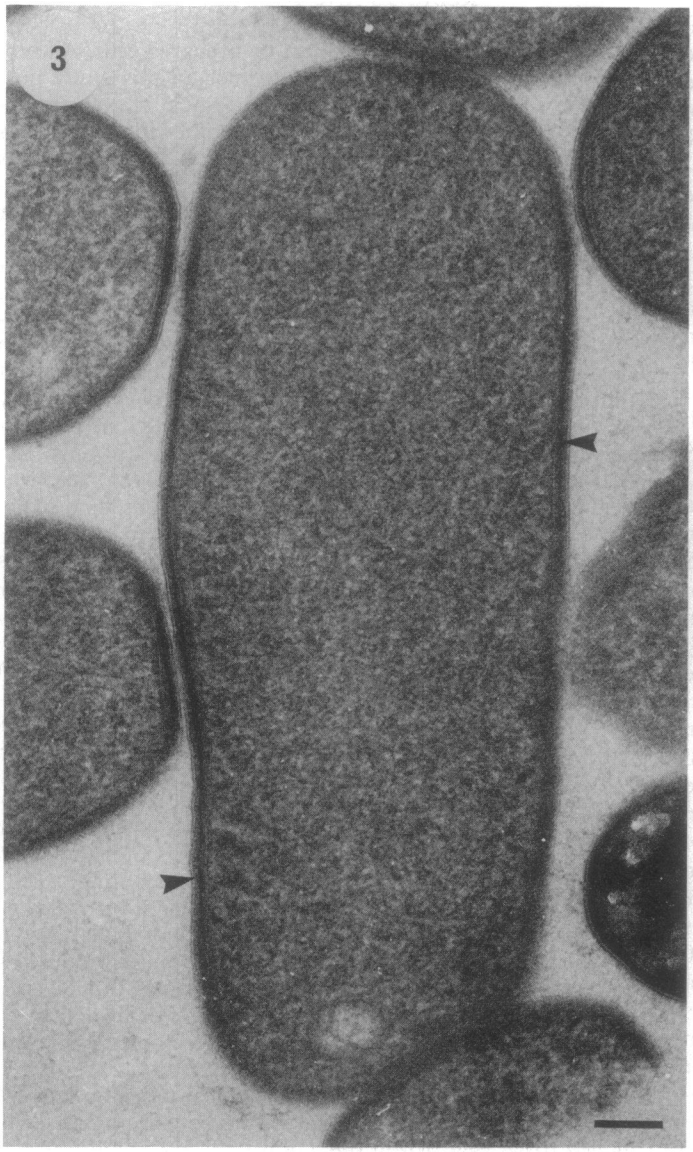
3

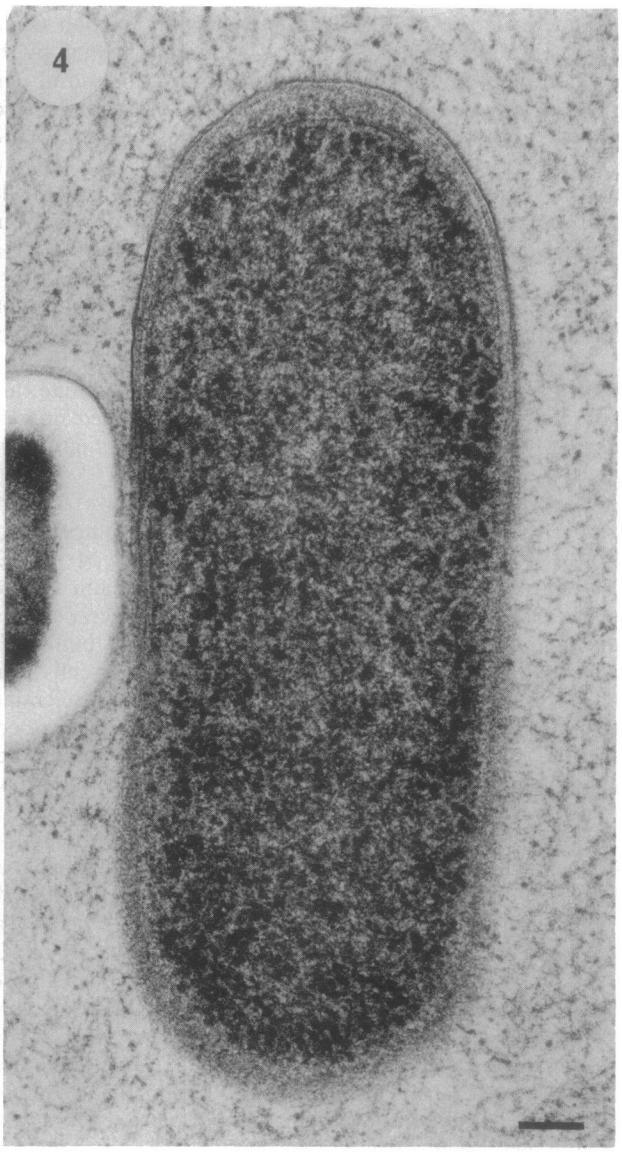
4

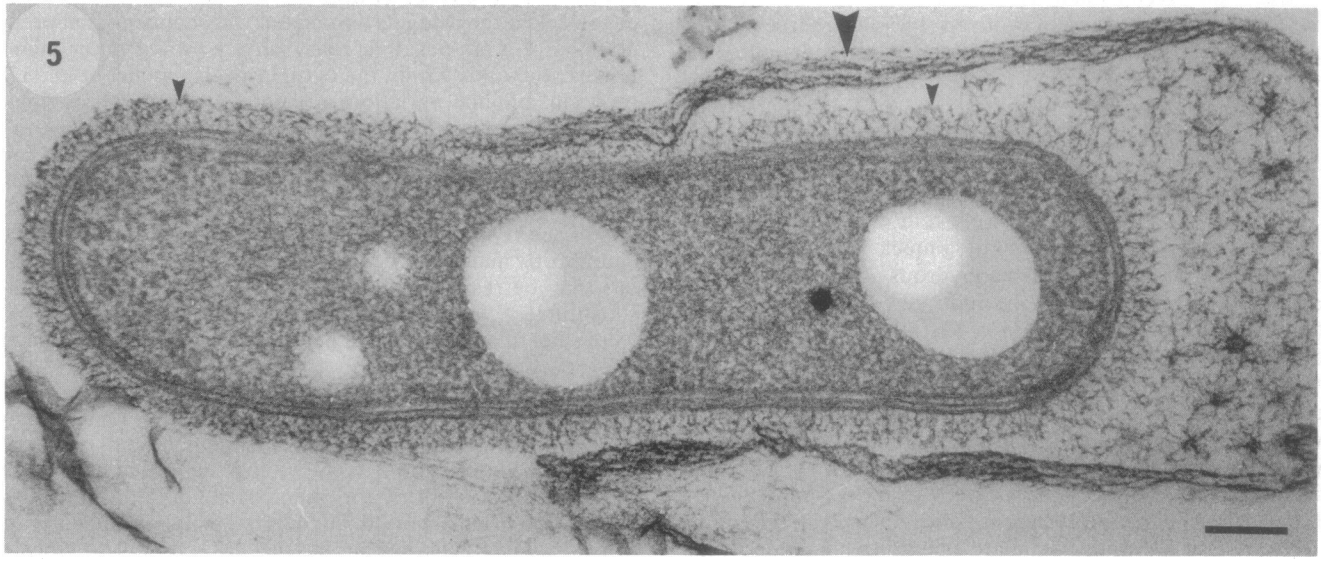
5

also Fig. 18). The trilaminar or double-track appearance of the outer membrane is caused by the deposition of uranyl ions and osmium complexes onto the charged head groups of the phospholipids, the phosphoryl groups of lipopolysaccharides (19), a limited number of carboxyl groups from lipopolysaccharide 3-deoxy-D-manno-octulosonate residues (20), and the acidic groups of exposed proteins. It is also possible that covalent linkage of osmium to select unsaturated carbon bonds (especially along the acyl chains) also occurs (26), although this hydrophobic portion of the membrane is known to exclude aqueous metal ions and is, consequently, more translucent than the hydrophilic faces (11). In the absence of heavy-metal stains, as in cells imaged in STEM mode by ratio contrast, the double track has not been observed (24).

In all cells examined, we believe the higher contrast observed in the outer face of the outer membrane compared with the inner face is a direct result of the natural partitioning of lipopolysaccharide exclusively in the outer face while phospholipids reside mostly on the inner face. Thus, the asymmetry of staining in the outer leaflet of the outer membrane reflects greater association of heavy metals such as osmium and uranyl ions with the lipopolysaccharide in this region (22) and confirms that the outer membrane lipid asymmetry has been retained during processing.

(ii) Periplasms. The periplasmic gel first observed by Hobot et al. (24) in *E. coli* B cells was 13 nm wide. Similar electron-dense regions have been observed in frozen-hydrated thin sections of *E. coli* F470 and 21409 and *Yersinia enterocolitica* Ye75R (1). In the *E. coli* K-12 cells examined in our present study (Fig. 6), the gel was ca. 14 nm in width. Often, adjacent membrane leaflets were so tightly appressed to this gel as to render them indistinguishable even by optical densitometry (22, 23), suggesting that cellular osmolarity had not been disturbed during processing and that the periplasm was chemically stabilized while in its fully extended or hydrated form. Thick periplasmic gels ranging from 10.6 to 14.3 nm in width were also observed in *E. coli* K30 and His 1, *A. salmonicida*, *C. fetus*, *P. mirabilis*, *P. putida*, *H. pleuropneumoniae*, and *P. multocida*.

A periplasmic gel was not apparent in all genera examined. *L. discophora* (Fig. 5 and see Fig. 17) and *C. crescentus* (see Fig. 11 and 12) possessed thinner peptidoglycan layers (3.4 and 4.8 nm, respectively) within an electron-translucent periplasmic space, reminiscent of conventionally prepared cells (11, 22). Typically, envelope profiles of *P. aeruginosa* (Fig. 7) and *V. cholerae* (Fig. 8) were intermediate, with nodes of electron-dense material in contact with both inner and outer membranes yet not completely filling the periplasm.

(iii) Plasma membranes. All strains examined revealed plasma membranes similar in appearance—bilayers, ca. 11 nm wide, and of uniform width and electron density (see Fig. 18). Like the outer membrane, plasma membranes were apparent prior to poststaining, although the outer face of this membrane was often very tightly appressed to the periplasmic gel and difficult to observe as previously reported (22, 23). Only in *L. discophora*, *C. crescentus*, *P. aeruginosa*, and *V. cholerae* were both faces of this membrane clearly evident.

(iv) S layers. Regularly structured surface arrays have been difficult to preserve by electron microscopy as they often have specific ion requirements which are difficult to maintain during processing (11). Our freeze-substitution protocol preserved the S layers of *A. salmonicida* and *C. crescentus*. Conventional preparations of *A. salmonicida* (Fig. 2) show an irregular layer external to the outer membrane, a variable distance away from and often with no physical attachment to the outer membrane. When processed by freeze-substitution, this layer was ca. 16 nm in width and tightly apposed to the outer membrane (Fig. 10). In *A. salmonicida* 449 TM1, an isogenic kanamycin-resistant strain which does not possess a surface array, this additional layer was not visible (Fig. 9).

The S layer of *C. crescentus* CB15A was also apparent in profiles of freeze-substituted cells. In this case, it was seen as a periodic layer of 10-nm-wide knoblike particles extending ca. 16 nm from the outer membrane (Fig. 12). These values are slightly larger than those published for negatively stained preparations of this array after isolation (36). Previously, thin-section profiles of conventionally fixed CB15A cells required tannic acid for S-layer preservation although very little periodicity was shown (36). When an isogenic strain in which the S-layer gene has been deleted (CB15A KSAC) was freeze-substituted, the outer membrane was visualized as the bacterium's most external surface (Fig. 11).

(v) Capsules. Like S layers, visualization of bacterial CPS has been hampered by a lack of adequate preparatory methods. The highly hydrated polymers composing bacterial capsules collapse during the dehydration stages of conventional processing (11). This has been overcome by the addition of polymer-specific antisera (31), lectins (12), or diamines such as lysine (27) which cross-link individual polymers, thereby minimizing their collapse during dehydration and resulting in retention of some structure. Unfortunately, these stabilized capsules are not always representative of native structure since their dimensions rarely correlate well with those determined by other methods such as freeze-etching or negative staining. Much of the resulting ultrastructure and mass of these stabilized capsules has been attributed to the presence of the stabilizing agent (11).

Recently, antigenicity in the capsule of *E. coli* K29 has been preserved by using gelatin-enrobed, glutaraldehyde-fixed cells dehydrated in dimethyl formamide in a progressive lowering-of-temperature protocol and embedding in Lowicryl K4M (8). In these cells, fibrous capsular material was observed extending 0.5 μm from the cell and native antigenicity was revealed by immunogold labeling.

Freeze-substitution is an alternate means of preserving this envelope component. Since chemical fixation and dehydration occur while polymers are frozen in their native conformation, distributed correctly about the cell, their fibrous nature is retained even in the absence of exogenous stabilizing agents. Capsules are among the most delicate bacterial structures known since their high water content makes them thixotrophic (11). Certainly, we have no guar-

FIG. 3. *E. coli* K-12 prepared by freeze-substitution. This section has not been poststained, and all contrast has been imparted by the substitution medium. Note the uniform appearance of the cytoplasm. Arrowheads indicate the periplasmic gel. Bar, 100 nm.

FIG. 4. Freeze-substituted *E. coli* K30 cell in which the extensive CPS is evident as the fibrous matrix surrounding the cell. Bar, 100 nm.

FIG. 5. *L. discophora* cell prepared by freeze-substitution. Note the presence of a capsule (small arrowhead) and, external to the capsule, a sheath (large arrowhead). Bar, 200 nm.

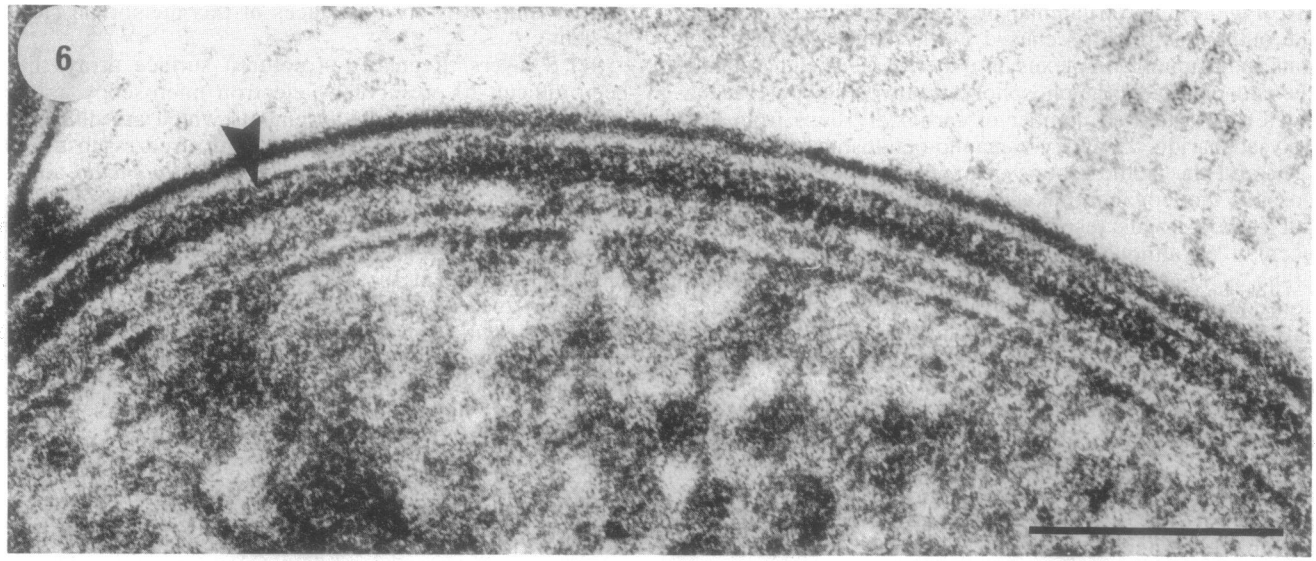
6

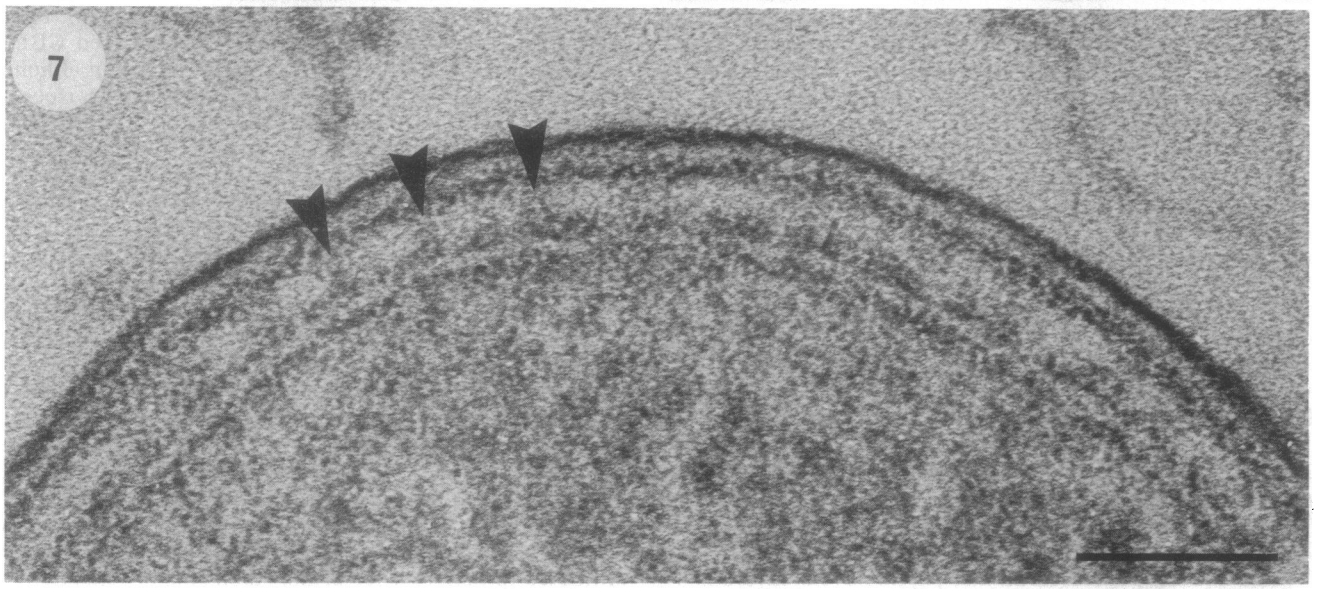
7

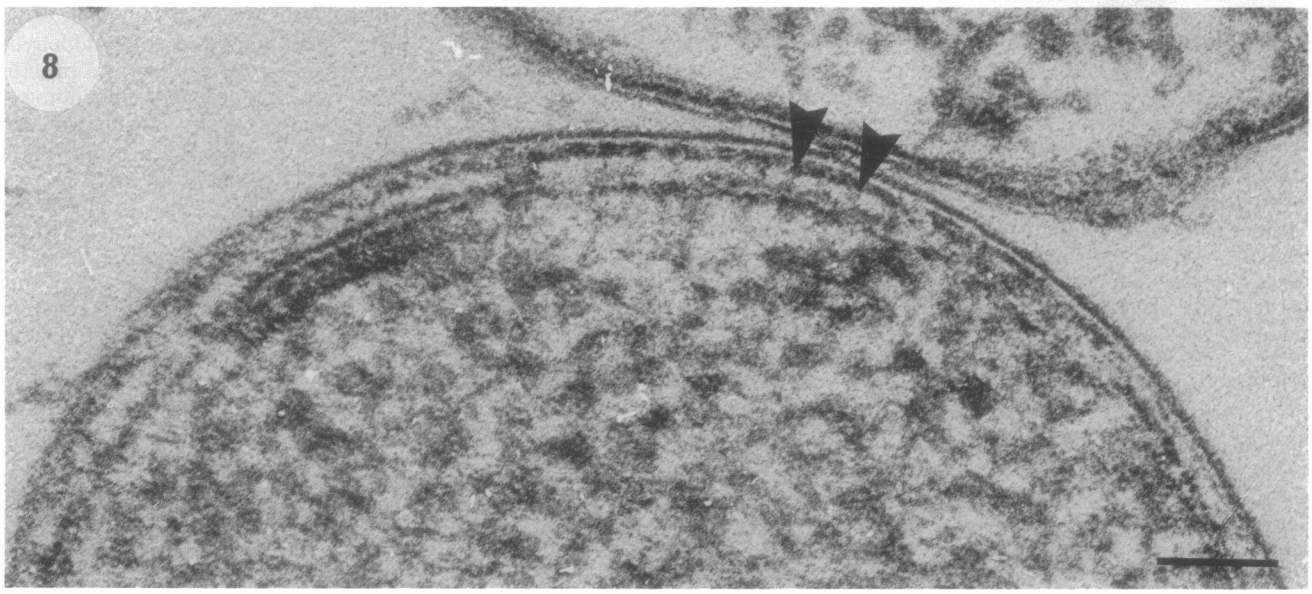
8

FIG. 6–8. High-magnification envelope profiles of cells prepared by freeze-substitution. Note the asymmetrically stained outer membranes and variable appearance of the peptidoglycan component within the periplasm.
FIG. 6. *E. coli* K-12. Arrowhead indicates the periplasmic gel. Bar, 50 nm.
FIG. 7. *P. aeruginosa* ATCC 9027. Arrowheads point to some of the nodes between outer and plasma membranes in both Fig. 7 and 8. Bar, 50 nm.
FIG. 8. *V. cholerae* CA401. Bar, 100 nm.

antee that rapid freezing will capture their exact physical expression on bacterial surfaces, but it must come close; cryofixation should not increase their energy load and induce a gel-to-liquid transition. Yet, some polymeric condensation may occur which could contribute to fiber thickness.

CPS was apparent on *E. coli* K30 (Fig. 13), *E. coli* His 1 (Fig. 14), *H. pleuropneumoniae* (Fig. 15), *P. mirabilis* (Fig. 16), and *L. discophora* (Fig. 5 and 17). Unlike cell membranes, visualization of this particular envelope component was enhanced by poststaining. From the encapsulated strains examined, it became clear that not all bacterial capsules exhibit identical structure. Variation in CPS polymer length, girth, and arrangement and distribution over the cell surface was evident between genera. The capsules of *H. pleuropneumoniae* and *L. discophora* appeared to be a random arrangement of fibers forming a netlike mesh which completely surrounded individual cells. The fibers composing the capsules of *E. coli* K30, *E. coli* His 1, and *P. mirabilis* were observed extending directly away perpendicular to the cell envelope in a more organized manner. Capsules exhibiting two polymeric arrangements have been reported for *E. coli* K1 (4) and for *Klebsiella pneumoniae* K and Chedid (33). In these cells, capsules are composed of an inner layer of densely packed fibers oriented perpendicular to the cell envelope and an outer layer of fine fibers which are more randomly oriented. Organization of capsular fibers into two distinct forms on cells prepared by freeze-substitution suggests that this technique may have captured the dynamic state of capsule turnover. Those fibers closely apposed to the outer membrane are bona fide capsule, whereas those

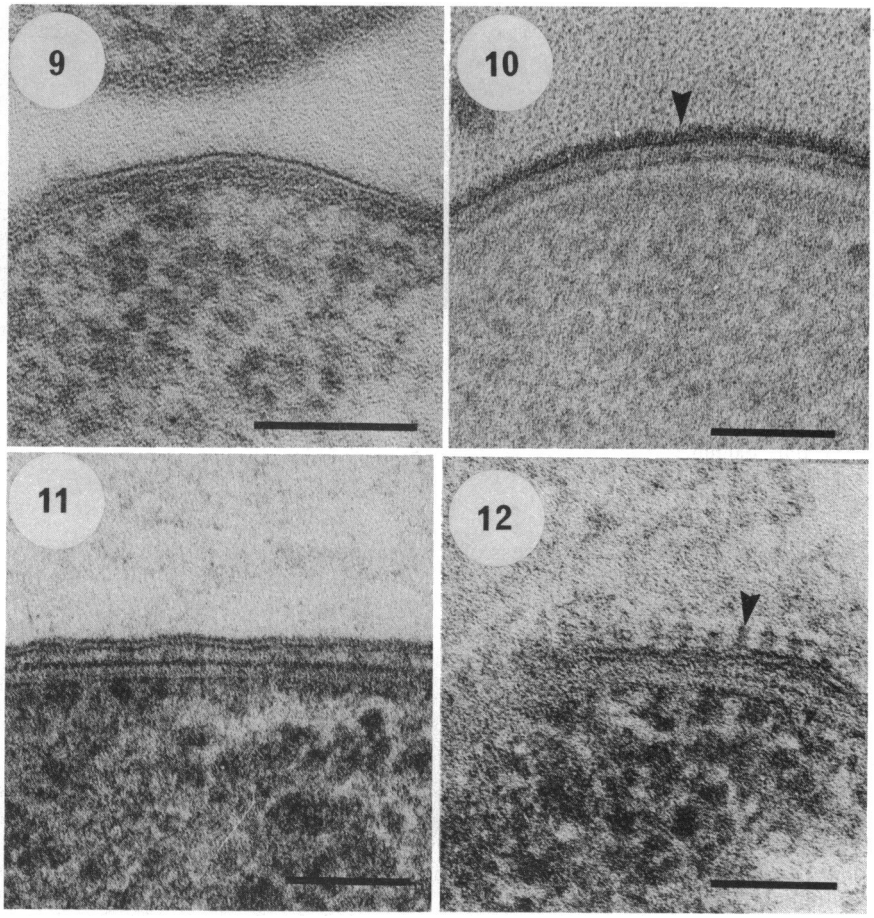

FIG. 9–12. Freeze-substituted preparations.
FIG. 9. Envelope profile of *A. salmonicida* 449 TM1 in which the A-layer is not expressed. Bar, 100 nm.
FIG. 10. Non-poststained envelope profile of *A. salmonicida* A450. Note the presence of an additional electron-dense layer external to the outer membrane (A-layer, arrowhead). Bar, 100 nm.
FIG. 11. *C. crescentus* CB15A KSAC which does not possess the S-layer gene. Bar, 100 nm.
FIG. 12. *C. crescentus* CB15A. Arrowhead indicates the S layer. Bar, 100 nm.

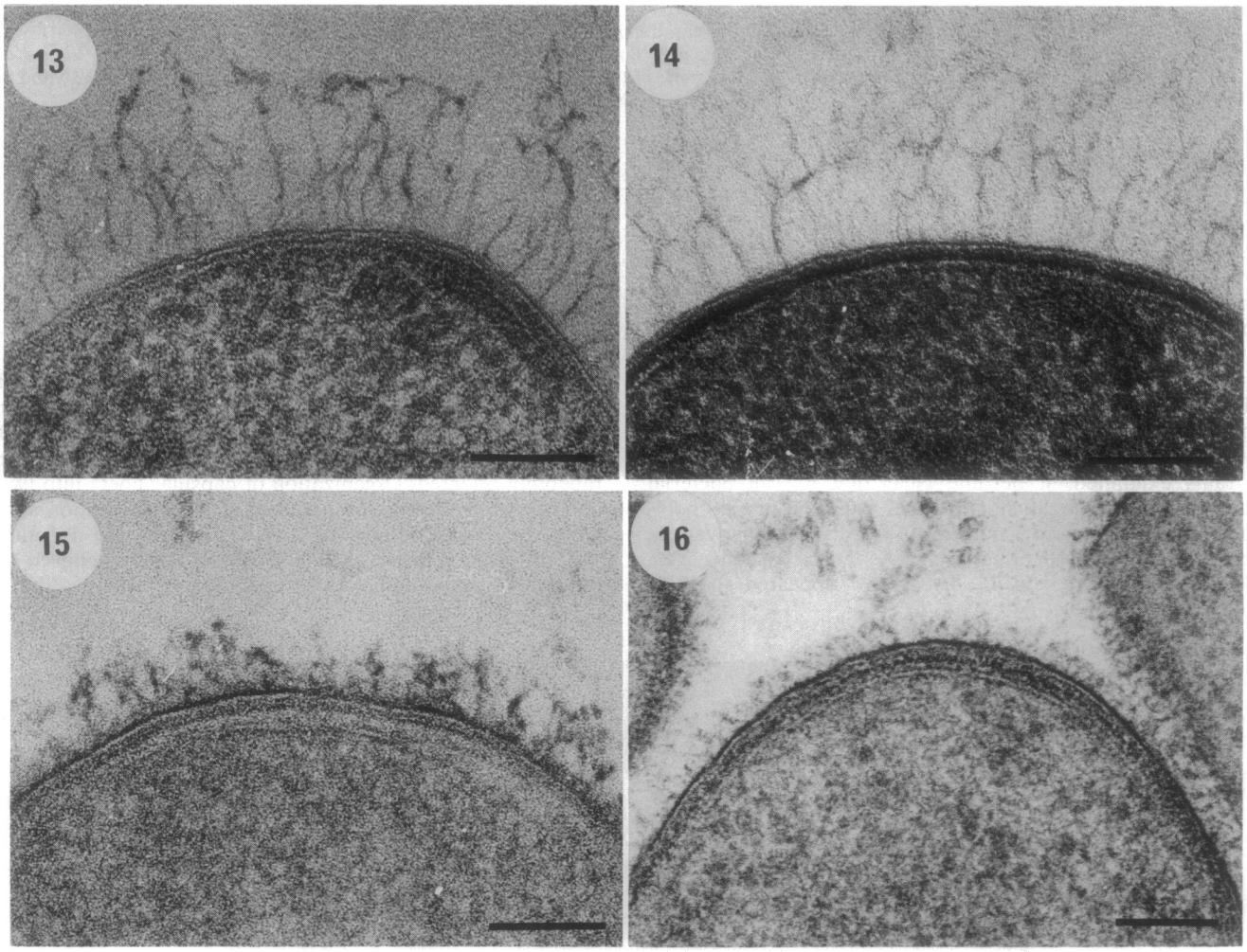

FIG. 13–16. Freeze-substituted envelope profiles of encapsulated cells. Note the variability in CPS polymer length, diameter, arrangement, and distribution between strains.
FIG. 13. *E. coli* K30. Bar, 100 nm.
FIG. 14. *E. coli* His 1. Bar, 100 nm.
FIG. 15. *H. pleuropneumoniae* CM5. Bar, 100 nm.
FIG. 16. *P. mirabilis* 2573. Bar, 100 nm.

more loosely arranged at the periphery are in the process of being sloughed off into the external milieu. Continued enzymatic hydrolysis would eventually solubilize these latter polymers. Complex capsular structures have also been found in freeze-substituted preparations of *Lactobacillus* species (13, 34) and *Vibrio vulnificus* (5). Together, these data suggest that the bacterial capsule exists in a variety of complex morphologic forms which may be readily visualized by freeze-substitution in the absence of exogenous stabilizing agents. Whitfield et al. (39) have used this technique to morphologically confirm the altered expression of CPS on mutants of *E. coli* O9:K30.

(vi) Sheaths. *L. discophora* is a sheathed bacterium noted for its ability to render soluble Mn into MnO_2 precipitates, a transition which occurs mostly in the matrix of the sheath and results in the formation of a mineralized cast (10). The sheath is a rugged polymeric matrix able to withstand this mineralization process. It can also withstand the rigors of conventional fixation and has been visualized as a diffuse, random arrangement of fibers which may extend over 500 nm above the cell surface (21). Freeze-substitution revealed a much more compact fabric for the sheath matrix which rarely exceeded 50 nm in thickness; the fibers were aligned and compacted along the longitudinal cell axis, were in contact with the underlying capsule polymers (the fibers external to but immediately adjacent to the outer membrane), and were deeply stained (Fig. 5 and 17). The good quality of cellular preservation (Fig. 5) suggests that the freeze-substitution image is natural.

Freeze-substitution versus conventional processing. We have previously reported that the technique of freeze-substitution with 2% osmium tetroxide and 2% uranyl acetate in anhydrous acetone is superior to conventional embedding processes for retaining cell ultrastructure (22, 23) and has revealed detail not previously observed by standard processing techniques (23a). The chemical combination of osmium tetroxide and uranyl acetate yields a high degree of contrast in the resulting thin sections so that poststaining is not required for visualization of most cell envelope constituents (Fig. 3). Although contrast in cell membranes and

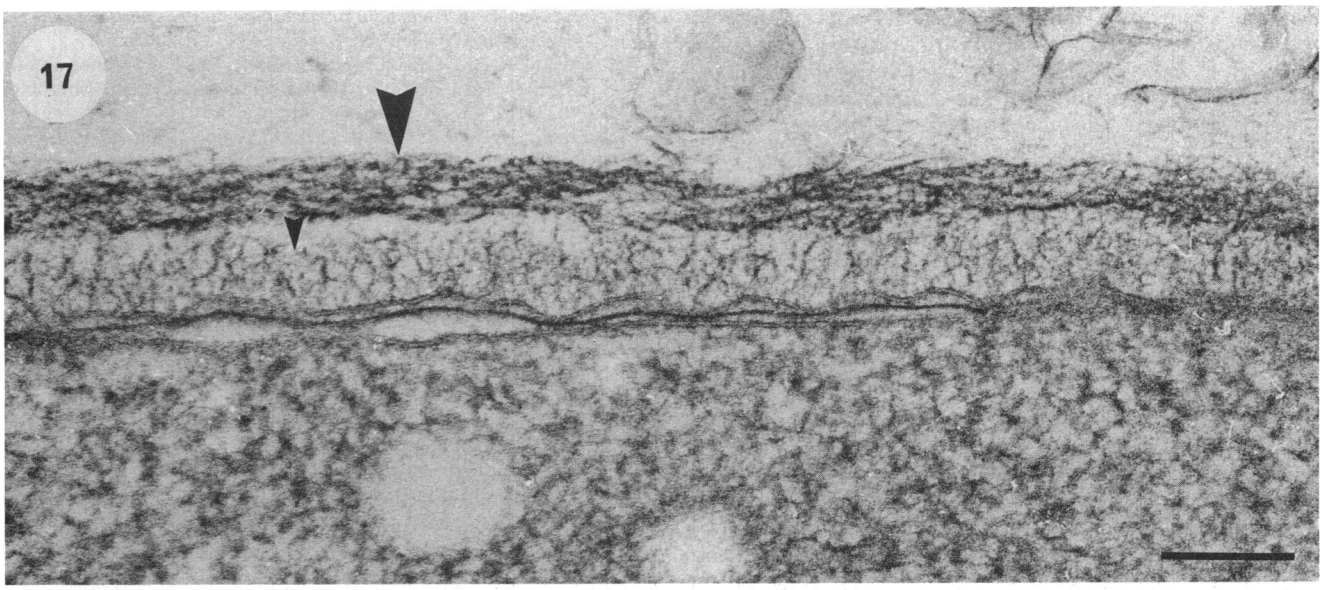

FIG. 17. Complex envelope profile of *L. discophora* in which both capsule (small arrowhead) and overlying sheath (large arrowhead) are visible. Bar, 200 nm.

cytoplasmic material may be enhanced by poststaining, little additional ultrastructural information is gained. This is an important observation for high-resolution microscopy since poststaining may actually obscure fine detail.

We have previously observed that cell envelope profiles vary as a function of the composition of the substitution medium itself (23). Our present study uses a single freeze-substitution regimen for comparison of a diverse range of gram-negative bacteria. In Fig. 18 we have diagrammatically summarized the resulting envelope profiles. It is apparent that although the cell envelope profile exhibited by *E. coli* K-12 is common among freeze-substituted gram-negative

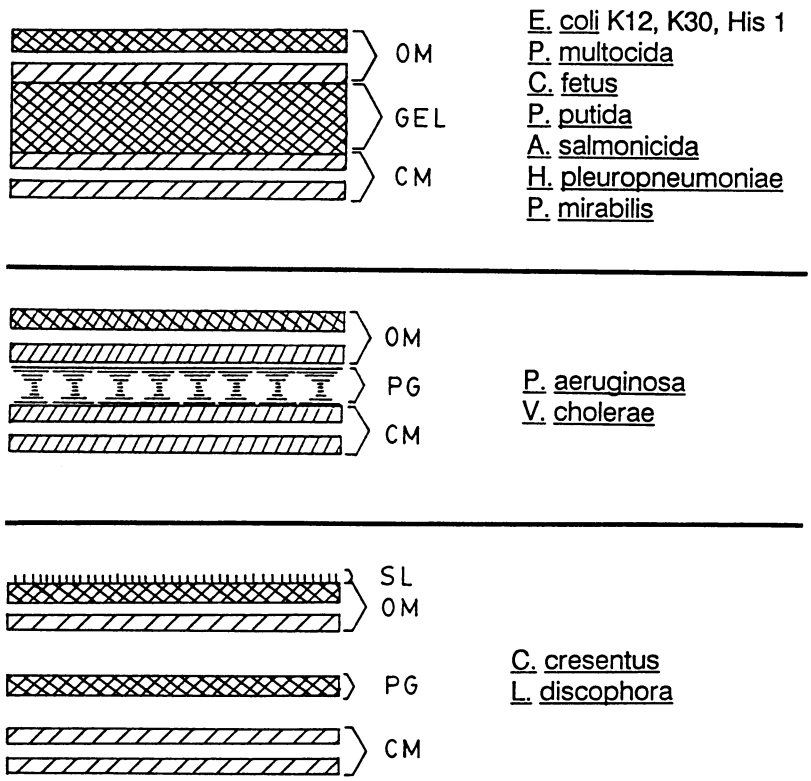

FIG. 18. Schematic representation of envelope profiles of the gram-negative bacteria examined in this study. OM, Outer membrane; GEL, periplasmic gel; CM, cytoplasmic membrane; PG, peptidoglycan; SL, S layer, sheath, and/or capsule.

bacteria, some gram-negative organisms present different freeze-substitution profiles and not all possess periplasmic gels, e.g., *P. aeruginosa*, *V. cholerae*, *L. discophora*, and *C. crescentus*. It is possible that subtle factors such as nutrition, growth phase, etc., could affect cell envelope composition, which could alter the expanse of the gel. It is also possible that these different profiles are inaccurate; perhaps some species freeze more poorly than *E. coli* or require different fixatives than *E. coli*. Indeed, given the biochemical variability of individual genera, it is most unlikely that a single processing protocol could satisfy all the preservative requirements. Yet, since we have preserved delicate capsules, S layers, and sheaths throughout a range of bacteria, it is our belief that these atypical profiles are an accurate representation.

Direct comparison of cells processed by both conventional means and by freeze-substitution (Fig. 1 and 3; Fig. 2 and 10) reiterates that structural information is lost or altered during standard chemical processing, directly reflecting the extent of biochemical leaching associated with this preparatory method (22). Ultimately, the quality of ultrastructure obtained in freeze-substituted specimens is dependent on the initial cryofixation process. Provided cells are frozen quickly enough to prevent specimen water from reorganizing into large regular crystalline lattices (i.e., vitrification is obtained), cell components will be fixed and dehydrated (the process of substitution) while maintained in their native conformation. The resulting cellular ultrastructure, therefore, should more closely resemble in vivo molecular arrangements. Freeze-substitution has revealed complex ultrastructural information in gram-negative cells in the absence of stabilizing agents and poststaining agents and as such offers an exciting tool for routine morphologic examination of bacteria. Additional structure will undoubtedly be revealed or redefined as more bacterial species are examined by this technique.

ACKNOWLEDGMENTS

We thank V. L. McKinley, S. Rosendahl, M. Jacques, J. Penner, J. Smit, S. G. Walker, T. J. Trust, and W. Ghiorse for contributing cultures for this study. We especially thank C. Whitfield for allowing us to use *E. coli* His 1, which was constructed in his laboratory.

Some of this research was accomplished while T.J.B. was a visiting scientist at the Biozentrum in Basel, Switzerland, with funding provided by the Swiss Science Foundation-Natural Sciences and Engineering Research Council (NSERC) of Canada Bilateral Research Program. During this period, E. Kellenberger, Department of Microbiology, Biozentrum, Basel, Switzerland, and E. Carlemalm, EMBL, Heidelberg, Federal Republic of Germany, provided interest, insight, and inspiration. Funding in Guelph was provided by a Medical Research Council of Canada operating grant to T.J.B. All microscopy was performed at the NSERC Guelph Regional STEM Facility located in the Department of Microbiology, the College of Biological Sciences, University of Guelph. This facility is partially maintained by an infrastructure grant from the Natural Sciences and Engineering Research Council of Canada.

REFERENCES

1. **Acker, G., D. Bitter-Suermann, U. Meier-Dieter, H. Peters, and H. Mayer.** 1986. Immunocytochemical localization of enterobacterial common antigen in *Escherichia coli* and *Yersinia enterocolitica* cells. J. Bacteriol. **168**:348–356.
2. **Adams, L. F., and W. C. Ghiorse.** 1985. Influence of manganese on growth of a sheathless strain of *Leptothrix discophora*. Appl. Environ. Microbiol. **49**:556–562.
3. **Aldrich, H. C.** 1989. Practical aspects of freeze-substitution. EMSA Bull. **19**:53–59.
4. **Amako, K., Y. Meno, and A. Takade.** 1988. Fine structures of the capsules of *Klebsiella pneumoniae* and *Escherichia coli* K1. J. Bacteriol. **170**:4960–4962.
5. **Amako, K., K. Okada, and S. Miake.** 1984. Evidence for the presence of a capsule in *Vibrio vulnificus*. J. Gen. Microbiol. **130**:2741–2743.
6. **Amako, K., and A. Takade.** 1985. The fine structure of *Bacillus subtilis* revealed by the rapid-freezing and substitution-fixation method. J. Electron Microsc. **34**:13–17.
7. **Bayer, M. E.** 1979. The fusion sites between outer membrane and cytoplasmic membrane of bacteria: their role in membrane assembly and virus infection, p. 167–202. *In* M. Inouye (ed.), Bacterial outer membranes: biogenesis and functions. John Wiley & Sons, Inc., New York.
8. **Bayer, M. E., E. Carlemalm, and E. Kellenberger.** 1985. Capsule of *Escherichia coli* K29: ultrastructural preservation and immunoelectron microscopy. J. Bacteriol. **162**:985–991.
9. **Bayer, M. H., G. P. Costello, and M. Bayer.** 1982. Isolation and partial characterization of membrane vesicles carrying markers of membrane adhesion sites. J. Bacteriol. **149**:758–767.
10. **Beveridge, T. J.** 1989. Metal ions and bacteria, p. 1–29. *In* T. J. Beveridge and R. J. Doyle (ed.), Metal ions and bacteria. John Wiley & Sons, Inc., New York.
11. **Beveridge, T. J.** 1981. Ultrastructure, chemistry, and function of the bacterial wall. Int. Rev. Cytol. **72**:229–317.
12. **Birdsell, D. C., R. J. Doyle, and M. Morgenstern.** 1975. Organization of teichoic acid in the cell wall of *Bacillus subtilis*. J. Bacteriol. **121**:726–734.
13. **Cook, R. L., R. J. Harris, and G. Reid.** 1988. Effect of culture media and growth phase on the morphology of lactobacilli and on their ability to adhere to epithelial cells. Curr. Microbiol. **17**:159–166.
14. **Cope, G. H., and M. A. Williams.** 1967. Quantitative studies on neutral lipid preservation in electron microscopy. J. R. Microsc. Soc. **88**:259–267.
15. **Cope, G. H., and M. A. Williams.** 1969. Quantitative studies on the preservation of choline and ethanolamine phosphatides during tissue preparation for electron microscopy. I. Glutaraldehyde, osmium tetroxide, araldite methods. J. Microsc. **90**:31–46.
16. **Cope, G. H., and M. A. Williams.** 1969. Quantitative studies on the preservation of choline and ethanolamine phosphatides during tissue preparation for electron microscopy. II. Other preparatory methods. J. Microsc. **90**:47–60.
17. **Dubochet, J., A. W. McDowall, B. Menge, E. N. Schmid, and K. G. Lickfeld.** 1983. Electron microscopy of frozen-hydrated bacteria. J. Bacteriol. **155**:381–390.
18. **Escaig, J.** 1982. New instruments which facilitate rapid freezing at 83°K and 6°K. J. Microsc. **126**:221–229.
19. **Ferris, F. G., and T. J. Beveridge.** 1986. Site specificity of metallic ion binding in *Escherichia coli* K12 lipopolysaccharide. Can. J. Microbiol. **32**:52–55.
20. **Ferris, F. G., and T. J. Beveridge.** 1986. Physicochemical roles of soluble metal cations in the outer membrane of *Escherichia coli* K12. Can. J. Microbiol. **32**:594–601.
21. **Ghiorse, W. C.** 1984. Biology of iron- and manganese-depositing bacteria. Annu. Rev. Microbiol. **38**:15–50.
22. **Graham, L. L., and T. J. Beveridge.** 1990. Evaluation of freeze-substitution and conventional embedding protocols for routine electron microscopic processing of eubacteria. J. Bacteriol. **172**:2141–2149.
23. **Graham, L. L., and T. J. Beveridge.** 1990. Effect of chemical fixatives on accurate preservation of *Escherichia coli* and *Bacillus subtilis* structure in cells prepared by freeze-substitution. J. Bacteriol. **172**:2150–2159.

23a. **Graham, L. L., R. Harris, and T. J. Beveridge.** 1989. Bacterial ultrastructure revealed by freeze-substitution. Proc. Microsc. Soc. Can. **16**:58–59.

24. **Hobot, J. A., E. Carlemalm, W. Villiger, and E. Kellenberger.** 1984. Periplasmic gel: new concept resulting from the reinvestigation of bacterial cell envelope ultrastructure by new methods. J. Bacteriol. **160**:143–152.
25. **Hobot, J. A., W. Villiger, J. Escaig, M. Maeder, A. Ryter, and E. Kellenberger.** 1985. Shape and fine structure of nucleoids ob-

served on sections of ultrarapidly frozen and cryosubstituted bacteria. J. Bacteriol. **162**:960–971.
26. **Horobin, R. W.** 1982. Histochemistry: an explanatory outline of histochemistry and biophysical staining, p. 311. Butterworths, Toronto.
27. **Jacques, M., and L. Graham.** 1989. Improved preservation of bacterial capsule for electron microscopy. J. Electron Microsc. Tech. **11**:167–169.
28. **Kay, W. W., J. T. Buckley, E. E. Ishiguro, B. M. Phipps, J. P. L. Monette, and T. J. Trust.** 1981. Purification and disposition of a surface protein associated with virulence of *Aeromonas salmonicida*. J. Bacteriol. **147**:1077–1084.
29. **Kellenberger, E.** 1990. The "Bayer bridges" confronted with results from improved electron microscopy methods. Mol. Microbiol. **4**:697–705.
30. **Knoll, G., A. J. Verkleij, and H. Plattner.** 1987. Cryofixation of dynamic processes in cells and organelles, p. 258–271. *In* R. A. Steinbrecht and K. Zierold (ed.), Cryotechniques in biological electron microscopy. Springer-Verlag, New York.
31. **Mackie, E. B., K. N. Brown, J. Lam, and J. W. Costerton.** 1979. Morphological stabilization of capsules of group B streptococci, types Ia, Ib, II, and III, with specific antibody. J. Bacteriol. **138**:609–617.
32. **McLean, R. J. C., J. Downey, L. Clapman, and J. C. Nickel.** 1990. A simple technique for studying struvite crystal growth in vitro. Urol. Res. **18**:39–43.
33. **Meno, Y., and K. Amako.** 1990. Morphological evidence for penetration of anti-O antibody through the capsule of *Klebsiella pneumoniae*. Infect. Immun. **58**:1421–1428.
34. **Reid, G., R. L. Cook, R. J. Harris, J. D. Rousseau, and H. Lawford.** 1988. Development of a freeze substitution technique to examine the structure of *Lactobacillus casei* GR-1 grown in agar and under batch and chemostat culture conditions. Curr. Microbiol. **17**:151–158.
35. **Reynolds, E. S.** 1963. Use of lead citrate as a stain in electron microscopy. Cell Biol. **17**:208–213.
36. **Smit, J., D. A. Grano, R. M. Glaeser, and N. Agabian.** 1981. Periodic surface array in *Caulobacter crescentus*: fine structure and chemical analysis. J. Bacteriol. **146**:1135–1150.
37. **Umeda, A., Y. Ueki, and K. Amako.** 1987. Structure of the *Staphylococcus aureus* cell wall determined by the freeze-substitution method. J. Bacteriol. **169**:2482–2487.
38. **Weibull, C., A. Christiansson, and E. Carlemalm.** 1983. Extraction of membrane lipids during fixation, dehydration and embedding of *Acholeplasma laidlawii* cells for electron microscopy. J. Microsc. **129**:201–207.
39. **Whitfield, C., G. Schoenhals, and L. Graham.** 1989. Mutants of *Escherichia coli* O9:K30 with altered synthesis and expression of the capsular K30 antigen. J. Gen. Microbiol. **135**:2589–2599.